Self-Assembly of Metal-Ion-Responsive Supramolecular Coordination Complexes and Their Photophysical Properties

Zuoli He,[a,b,*] Meng Li,[c] Wenxiu Que,[a,*] and Peter J. Stang[b,*]

a. Electronic Materials Research Laboratory, International Center for Dielectric Research, Key Laboratory of the Ministry of Education, School of Electronic and Information Engineering, Xi'an Jiaotong University, Xi'an 710049, Shaanxi, People's Republic of China

b. Department of Chemistry, University of Utah, 315 South 1400 East, Room 2020, Salt Lake City, Utah 84112, United States

c. Center for Self-assembly and Complexity (CSC), Institute for Basic Science (IBS), Pohang, 37363, Republic of Korea

Email address: : zuoli.he@utah.edu, wxque@xjtu.edu.cn; stang@chem.utah.edu

Table of Contents

General information 1

Experimental Section 2

Synthesis of 5,5'-bis(pyridin-4-ylethynyl)-2,2'-bipyridine (PYP) 2

Synthesis of the trigonal 3-connector 2,4,6-tris(4-pyridyl)-1,3,5-triazine(TPT) 5

Supporting Figures 6

Figure S1. ^1H NMR spectrum of S1 in $CDCl_3$. 6

Figure S2. ^{13}C NMR spectrum of S1 in $CDCl_3$. 7

Figure S3. ^1H NMR spectrum of S2 in $CDCl_3$. 8

Figure S4. ^{13}C NMR spectrum of S2 in $CDCl_3$. 9

Figure S5. ^1H NMR spectrum of S3 in $CDCl_3$. 10

Figure S6. ^{13}C NMR spectrum of S3 in $CDCl_3$. 11

Figure S7. ^{1}H NMR spectrum of PYP in $CDCl_3$. 12

Figure S8. ^{13}C NMR spectrum of PYP in $CDCl_3$. 13

Figure S9**.** ESI-MS spectrum of PYP....14

Figure S10. X-ray structures of the 5,5'-bis(pyridin-4-ylethynyl)-2,2'-bipyridine (PYP)..15

Figure S11. ^{1}H NMR spectrum of TPT in CD_2Cl_2. 16

Figure S12. ^{1}H NMR spectra of ligands (PYP and TPT), acceptor, and self-assembled square-like SCC-I and trigonal prisms-like SCC-II in CD_2Cl_2. 17

Figure S13. ^{1}H NMR spectrum of square-like SCC-I in acetone-*d*$_6$....18

Figure S14. ^{31}P {^{1}H} NMR spectrum of square-like SCC-I in acetone-*d*$_6$....19

Figure S15. ^{1}H NMR spectrum of trigonal prisms-like SCC-II in $CD_2Cl_{2.}$ 20

Figure S16. ^{31}P {^{1}H} NMR spectrum of trigonal prisms-like SCC-II in acetone-*d*$_{6.}$....21

Figure S17. Proposed structure of the SCC-I (a-d) and SCC-II(e-h) as obtained by Materials Studio via "clean" utility to gain good molecular geometries when added force center. 22

Figure S18. Absorption spectra of different ligands and self-assembled square-like SCC-I and trigonal prisms-like SCC-II (5×10^{-5} M in DCM). 23

Figure S19. Fluorescence emission spectra (λ_{ex} = 340 nm) spectra of different ligands and self-assembled square-like SCC-I and trigonal prisms-like SCC-II(5×10^{-5} M in DCM)....24

Figure S20. ^{31}P {^{1}H} NMR spectra of Zn^{2+} ion-responsive self-assembled square-like SCC-I in acetone-*d*$_6$ with different amount of $Zn(ClO_4)_2$ dissolved in acetone-*d*$_6$. 25

Figure S21. ^{31}P {^{1}H} NMR spectrum of Zn^{2+} ion-responsive self-assembled trigonal prisms-like SCC-II in acetone-*d*$_6$ (Zn^{2+} : SCCs = 1:1)....26

Figure S22. Fluorescence emission spectra (λ_{ex} = 340 nm) spectra of metal-ion-responsive self-assembled SCCs, a and b: Ni^{2+} and Zn^{2+} -square-like SCC-I; c and d Ni^{2+} and Zn^{2+} -trigonal prisms-like SCC-II in DCM(5×10^{-5} M in DCM). 27

Figure S23. Simulated isotope distribution for species $[Ni@SCC\text{-}I - 4PF_6]^{4+}$ {m/z=962.2207}(bottom) and experimental isotope distribution for $[Ni@SCC\text{-}I - 4PF_6]^{4+}${m/z=962.2190} (top). 28

Figure S24. Simulated isotope distribution for species [Ni@SCC-II - 6PF$_6$]$^{6+}${m/z=886.7040}(bottom) and experimental isotope distribution for [Ni@SCC-II - 6PF$_6$]$^{6+}${m/z=886.7078} (top). 29

Figure S25. Absorption spectra of Ag$^+$ ion-responsive self-assembled SCCs: a, square-like SCC-I; b, trigonal prisms-like SCC-II in DCM(5×10^{-5} M in DCM, metal ion : SCCs = 0~3 eq). 30

Figure S26. Absorption spectra of Nd^{3+} ion-responsive self-assembled SCCs: a, square-like SCC-I; b, trigonal prisms-like SCC-II in DCM (5×10^{-5} M in DCM, metal ion : SCCs = 0~3 eq). 31

Figure S27. Absorption spectra of Eu^{3+} ion-responsive self-assembled SCCs: a, square-like SCC-I; b, trigonal prisms-like SCC-II in DCM(5×10^{-5} M in DCM, metal ion : SCCs = 0~3 eq). 32

Figure S28. Absorption spectra of Tb^{3+} ion-responsive self-assembled SCCs: a, square-like SCC-I; b, trigonal prisms-like SCC-II in DCM. (5×10^{-5} M in DCM, metal ion : SCCs = 0~2 eq). 33

Figure S29. Absorption spectra of Zn^{2+} and Ni^2+ion-responsive self-assembled SCCs: a, square-like SCC-I; b, trigonal prisms-like SCC-II in DCM. (5×10^{-5} M in DCM, metal ion : SCCs = 2 eq). 34

Figure S30. Absorption spectra of different metal ion-responsive self-assembled SCCs: a, square-like SCC-I; b, trigonal prisms-like SCC-II in DCM. (5×10^{-5} M in DCM, metal ion : SCCs = 2 eq). 35

Supporting Table 36

Table 1. Crystal data and structure refinement for PYP (pjs249). 36

References 37

General information

All chemicals were commercial available and used as it is without further purification. All solvent was dried over standard drying agents.[1] Deuterated solvent was purchased from Cambridge Isotope Laboratory (Andover, MA). Column chromatography was carried out using Silica 60A (particle size 35-70 μm, Fisher, UK) as the stationary phase, and thin layer chromatography (TLC) was performed on precoated silica gel plates (0.25 mm thick, 60 F254, Merck, Germany) and observed under a UV hand lamp at λ= 254 nm or λ= 365 nm. NMR spectra were recorded on a Varian Unity 300 MHz spectrometer. ^{1}H and ^{13}C NMR chemical shifts are reported relative to residual solvent signals, and ^{31}P{^{1}H} NMR chemical shifts are referenced to an external unlocked sample of 85% H_3PO_4 (δ 0.0) aqueous solution. Mass spectra for the compounds and metallacycles were recorded on a Micromass Quattro II triple-quadruple mass spectrometer using electrospray ionization (ESI) with a MassLynx operating system. UV-Vis absorption and fluorescence spectra were recorded on a Hitachi U-4100 and Hitachi F-7000 Spectrophotometer, respectively, in spectroanalyzed dichloromethane, acetone, and methanol (Fisher Scientific, US) at room temperature. The cuvette used in the experiments were 1 cm quartz cuvettes from Starna Cells. All samples were freshly prepared for each measurement.

Experimental Section

Synthesis of 5,5'-bis(pyridin-4-ylethynyl)-2,2'-bipyridine (PYP)

Synthesis of 5,5'-bis(pyridin-4-ylethynyl)-2,2'-bipyridine (PYP) is summarized in Scheme S1.

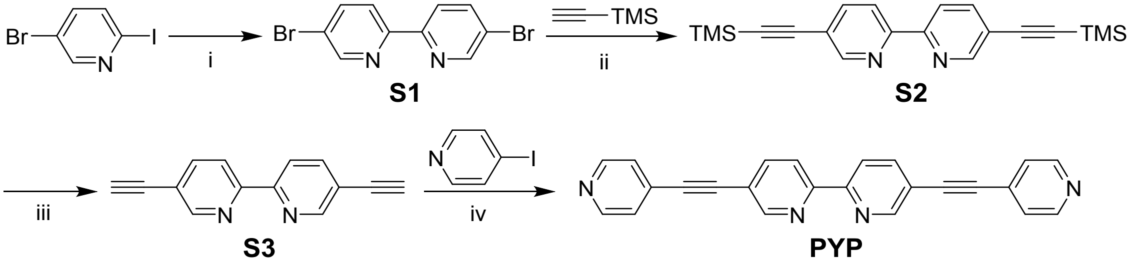

Scheme S1. Preparation of 5,5'-bis(pyridin-4-ylethynyl)-2,2'-bipyridine (PYP). Reagents and conditions: (i) 0.10 eq Pd(PPh$_3$)$_4$, 0.54 eq *n*-Bu$_6$Sn$_2$, toluene, 120 °C, reflux, 3 days, 82%; (ii) 0.10 eq Pd(PPh$_3$)$_4$, 0.05 eq CuI, toluene, NEt$_3$, 50 °C, reflux, overnight, 87%; (iii) 1.0 eq K$_2$CO$_3$, MeOH, THF, 4 hour, 90%; (iv) 0.20 eq Pd(PPh$_3$)$_4$, 0.05 eq CuI, THF, NEt$_3$, 60 °C, reflux, 2 days, 62%.

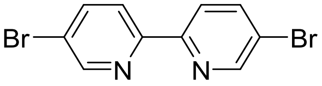

S1

5,5'-dibromo-2,2'-bipyridine (S1) was prepared following previous report.[2]

5-Bromo-2-iodopyridine (2.20 g, 7.75 mmol), Pd(PPh$_3$)$_4$ (240 mg, 0.19 mmol), and n-Bu$_6$Sn$_2$ (2.42 g, 4.17 mmol) was dissolved in freshly distilled toluene (40 mL) and stirred under nitrogen atmosphere for 72 h at 115 °C. The solvent was then evaporated, and chloroform was added to dissolve the crude product. The chloroform solution was washed with brine and dried over anhydrous MgSO$_4$. After removing the solvent, the resulting residue was eluted with CHCl$_3$-CH$_3$OH (99.9 : 0.1) through silica gel flash chromatography to give 5,5'-dibromo-2,2'-bipyridine (S1) as a white solid (1.01 g, 82%). ^{1}H NMR (300 MHz, CDCl$_3$) δ 8.70 (m, 1H), 8.29 (d, *J* = 8.5, Hz, 1H), 7.93 (d, *J* = 8.5 Hz, 1H). ^{13}C NMR (75 MHz, CDCl$_3$) δ 153.90, 150.50, 139.81, 122.44, 121.66.

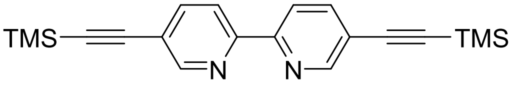

S2

5,5'-bis((trimethylsilyl)ethynyl)-2,2'-bipyridine (S2)was prepared following previous report.[2]

Trimethylsilylacetylene (4 mL, 28.1 mmol) was added to a degassed solution of S1 (3.0 g, 9.5 mmol) in a mixture of toluene (200 mL) and triethylamine (75 mL), and then Pd(PPh$_3$)$_4$ (0.555 g, 0.48 mmol, 5%) and CuI (0.27 g, 1.42 mmol, 15%) were added under the nitrogen atmosphere. The mixture was stirred at 60 °C overnight. The solution was removed under reduced pressure, and the residue was dissolved in CH_2Cl_2. After washing with an aqueous saturated solution of NH_4Cl and drying with $MgSO_4$, CH_2Cl_2 was evaporated and the remaining residue was eluted with CH_2Cl_2-MeOH (CH_2Cl_2 : MeOH 100:0 to 95:5) through silica gel flash chromatography to afford S2 as a pale yellow. Solid (3.0 g, 8.58 mmol, 89%). ^{1}H NMR (300 MHz, $CDCl_3$) δ 8.71 (s, 2H), 8.35 (d, *J* = 8.2 Hz, 2H), 7.86 (d, *J* = 8.2 Hz, 2H), 0.28 (s, 18H). ^{13}C NMR (75 MHz, $CDCl_3$) δ 154.38, 152.29, 140.05, 120.66, 101.97, 99.74, 77.68, 77.26, 76.84, 0.09.

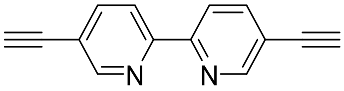

S3

5,5'-diethynyl-2,2'-bipyridine (S3) was also prepared by a modified procedure.[2]

5,5'-bis((trimethylsilyl)ethynyl)-2,2'-bipyridine (400 mg, 1.15 mmol) was dissolved in methanol : THF (1:1, 20 mL) and K_2CO_3 powder (200 mg, 1.45 mmol) was added. The mixture was stirred overnight at room temperature and the solvent was removed under vacuum, after which, the crude product was dissolved in CH_2Cl_2 (50 mL) and washed with brine for 3 times. The organic layer was treated with activated charcoal, dried over $MgSO_4$ and the solvent was removed under reduced pressure to give S3 as a brown yellow solid (200.5 mg, 86%) which was used as starting materials for next step. ^{1}H NMR (300 MHz, $CDCl_3$) δ 8.76 (d, *J* = 2.1 Hz, 2H), 8.39 (d, *J* = 8.3 Hz, 2H), 7.90 (d, *J* = 8.2 Hz, 2H), 3.30 (s, 2H). ^{13}C NMR (75 MHz, $CDCl_3$) δ 154.78, 152.51, 140.30, 120.82, 119.67, 81.89, 80.84.

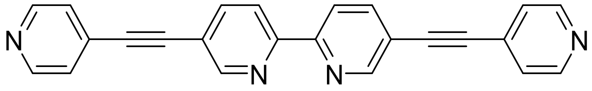

PYP

5,5'-bis(pyridin-4-ylethynyl)-2,2'-bipyridine (PYP) was prepared referring to the previous literature.[3]

5,5'-diethynyl-2,2'-bipyridine (400 mg, 1.97 mmol), 4-iodopyridine (2.05 g, 10 mmol), $Pd(PPh_3)_4$ (462.4 mg, 0.4 mmol) and CuI (19.0 mg, 0.1 mmol) were dissolved in freshly distilled THF (40 mL) and TEA (20 mL). After deoxygenation, the solution was kept at 60 °C for 3 days and then cooled down to room temperature. Activated carbon was added and the mixture was filtered over celite. The filtrate was absorbed onto SiO_2 and eluted through silica gel flash chromatography (CH_2Cl_2:CH_3OH 100:0 to 80:20) to afford crude ligand as a slightly yellow solid which was dissolved in a minimum volume of CH_2Cl_2 and precipitated by petroleum ether to obtain pure 5,5'-bis(pyridin-4-ylethynyl)-2,2'-bipyridine (PYP) as a yellow solid (437 mg, 62%). Purple crystals were obtained by slow vapor diffusion of diethyl ether into a CH_2Cl_2 solution of PYP over 7 days. ESI-MS: $[M+H]^+$ m/z

= 359.2. m.p. 256 - 260 °C (dec.). ^{1}H NMR (300 MHz, $CDCl_3$) δ 8.84 (d, *J* = 1.3 Hz, 2H), 8.65 (d, *J* = 4.4, 1.6 Hz, 4H), 8.48 (d, *J* = 8.5 Hz, 2H), 7.98 (d, *J* = 8.2 Hz, 2H), 7.42 (d, *J* = 6.1 Hz, 4H). ^{13}C NMR (75 MHz, $CDCl_3$) δ 154.91, 152.18, 150.16, 139.96, 130.84, 125.73, 121.03, 119.77, 91.13, 90.81.

Synthesis of the trigonal 3-connector 2,4,6-tris(4-pyridyl)-1,3,5-triazine(TPT)

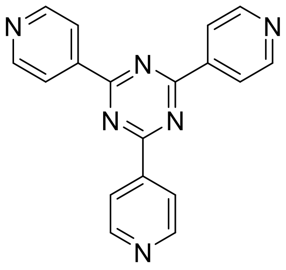

TPT

2,4,6-tris(4-pyridyl)-1,3,5-triazine(TPT) was prepared referring to the previous literature.[4]

18-crown-6 (500 mg, 1.9 mmol) and KOH (112.5 mg, 2.0 mmol) were dissolved in 10 mL of ethanol and stirred for 20 min. The solvent was removed under reduced pressure to obtain an oil product. To this oil, 4-cyanopyridine (5 g, 48 mmol) was added. The mixture was stirred at 200 °C. The color changed to red within a short period of time. After stirring at 200 °C for 6 h, the mixture was cooled down to room temperature, and then 60 mL of pyridine was added. Stirring the mixture for 5 min gave the fine crystal compound which was then filtrated and washed 2 times with pyridine (25 mL) and toluene (25 mL). The pale-red crystals were dissolved in 2 mol L^{-1} HCl (60 mL). After removing insoluble solid by filtration, pH value was adjusted to slight alkaline using concentrated NH_3 aqueous solution to give a pale-white powder which was then filtrated, washed with water, and dried in air to afford TPT (3.5 g, 70%). ^1H NMR (300 MHz, CD_2Cl_2) δ 8.92 (6H), 8.60 (6H).

Supporting Figures

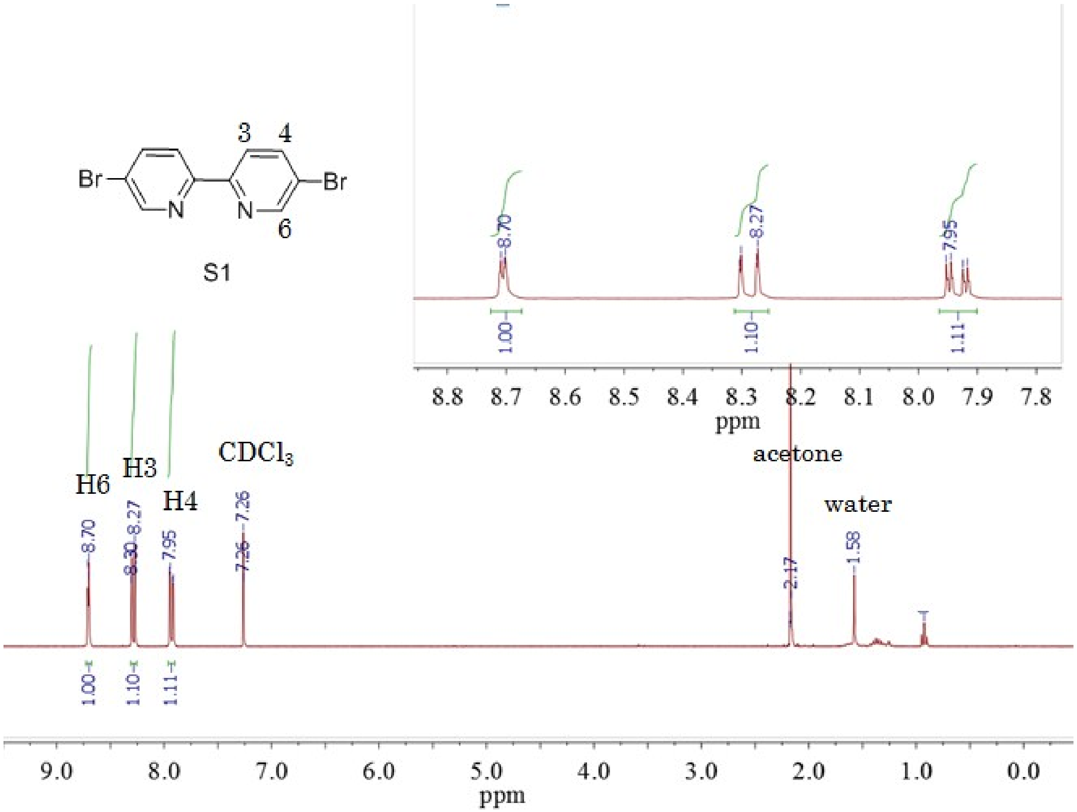

Figure S1. ^{1}H NMR spectrum of S1 in CDCl$_3$.

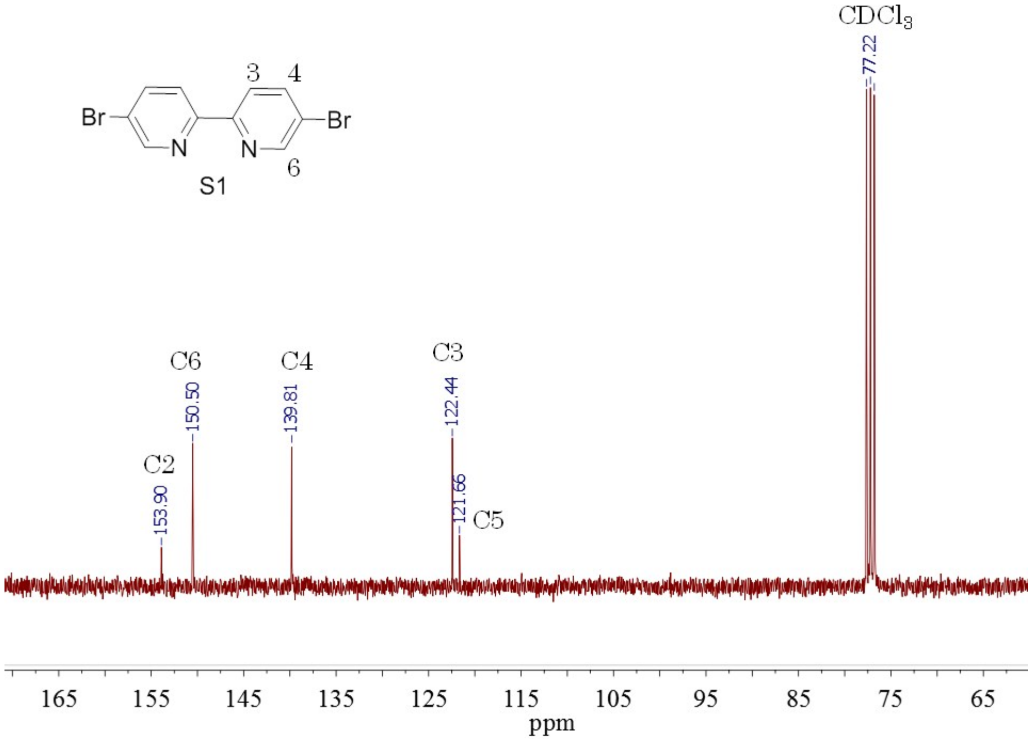

Figure S2. ${}^{13}C$ NMR spectrum of S1 in $CDCl_3$.

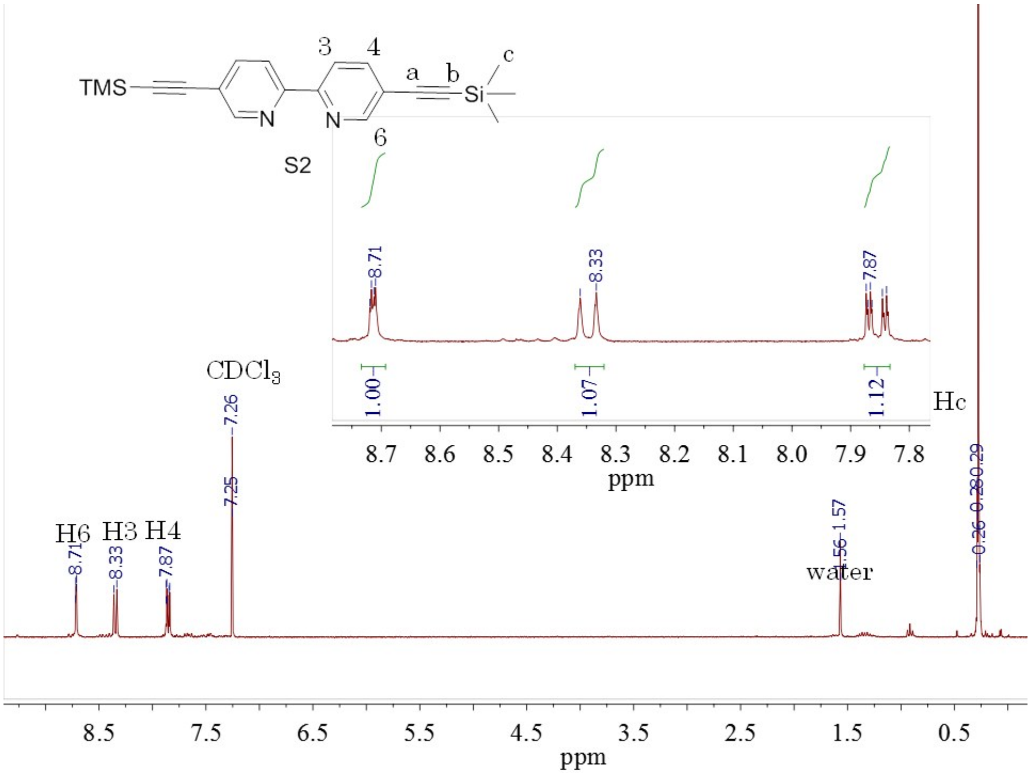

Figure S3. ^{1}H NMR spectrum of S2 in $CDCl_3$.

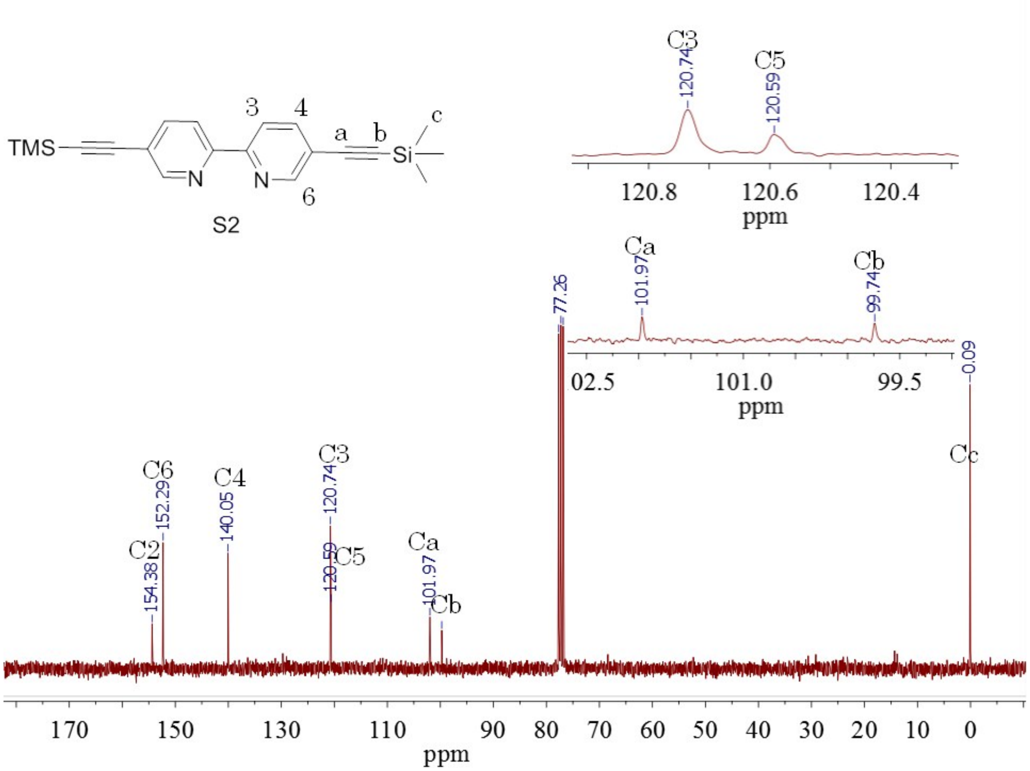

Figure S4. ^{13}C NMR spectrum of S2 in $CDCl_3$.

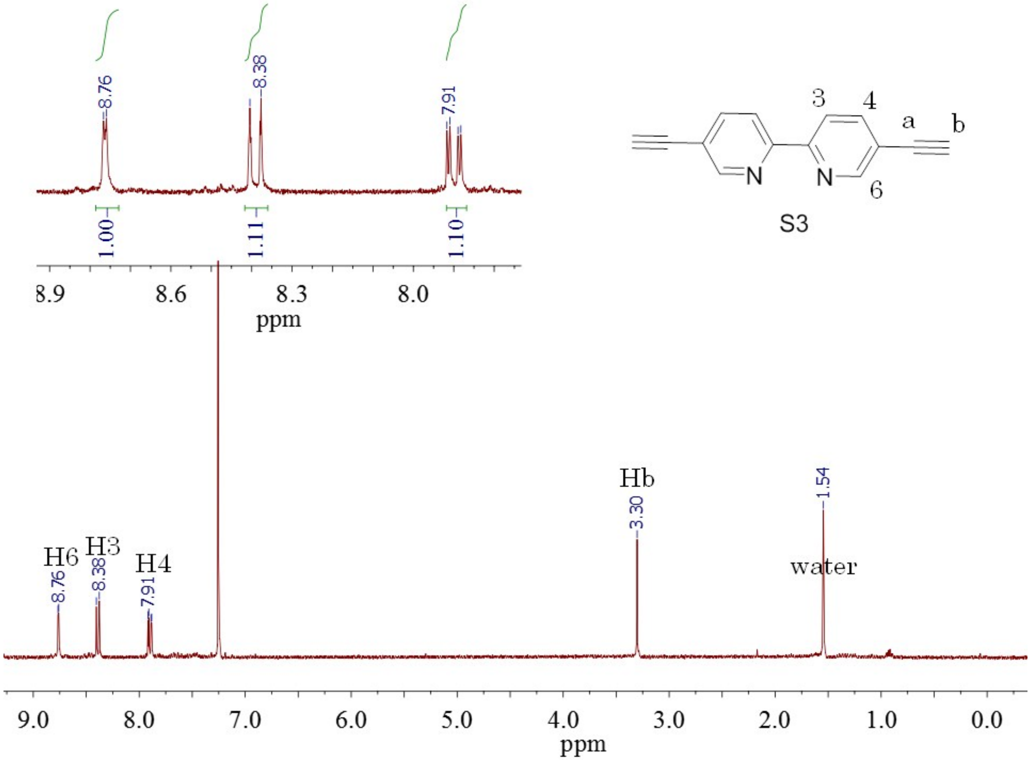

Figure S5. ^{1}H NMR spectrum of S3 in $CDCl_3$.

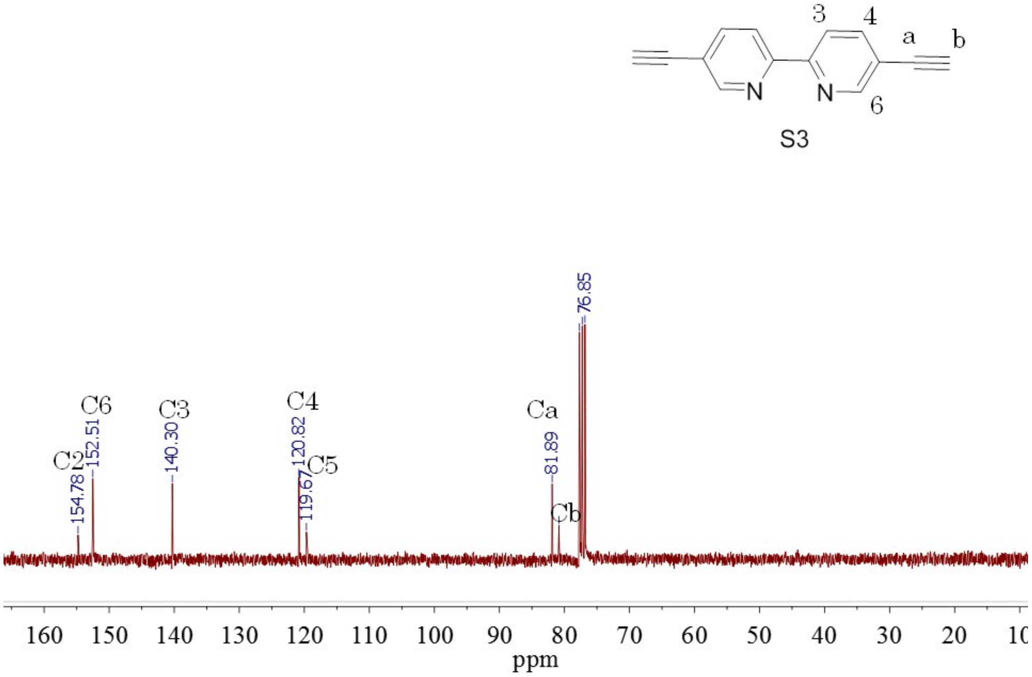

Figure S6. ^{13}C NMR spectrum of S3 in $CDCl_3$.

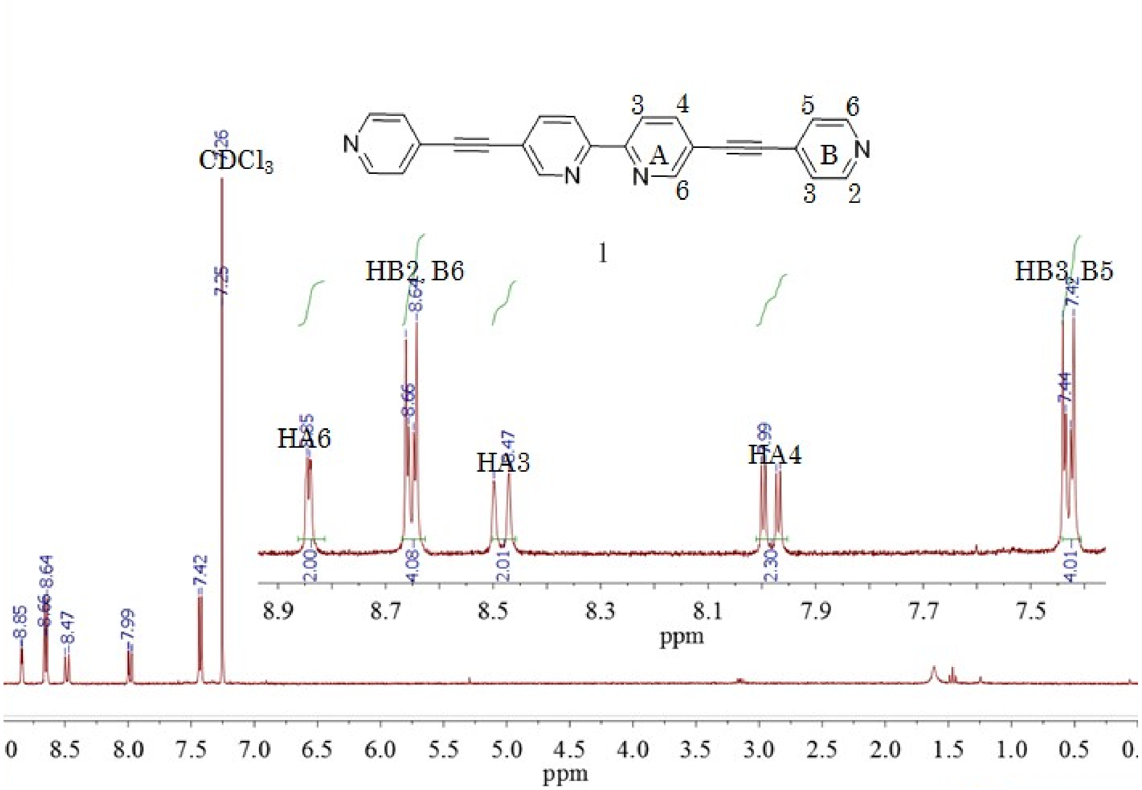

Figure S7. ^{1}H NMR spectrum of PYP in $CDCl_3$.

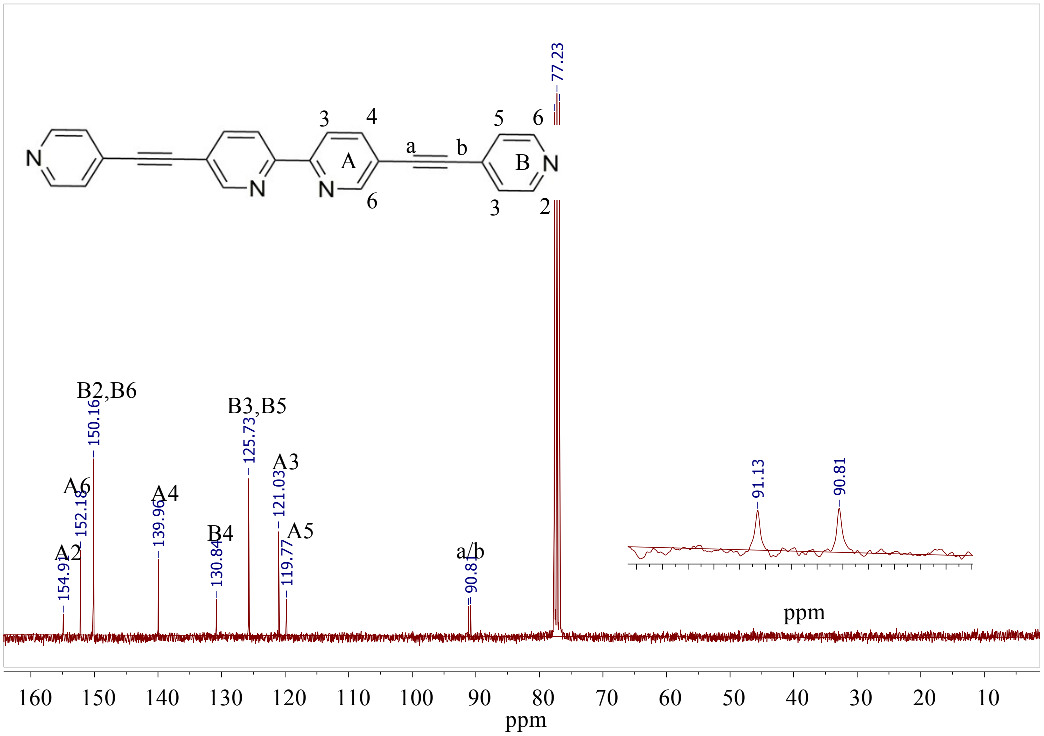

Figure S8. ^{13}C NMR spectrum of PYP in $CDCl_3$.

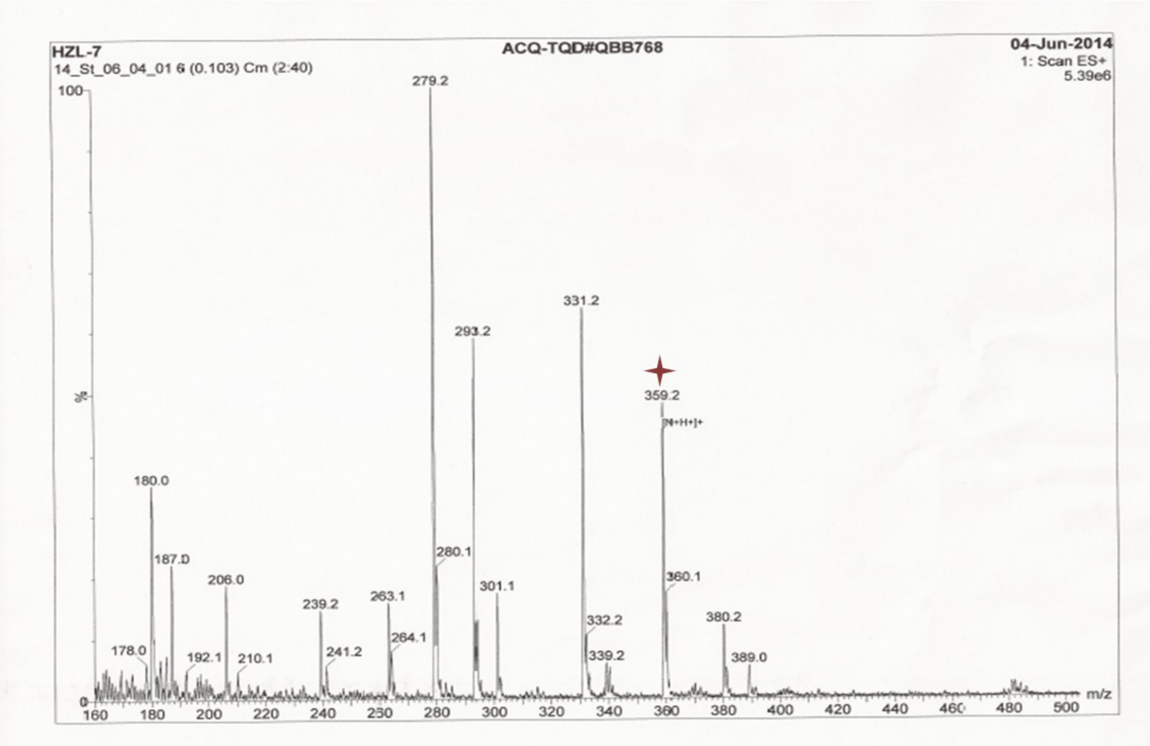

Figure S9. ESI-MS spectrum of PYP.

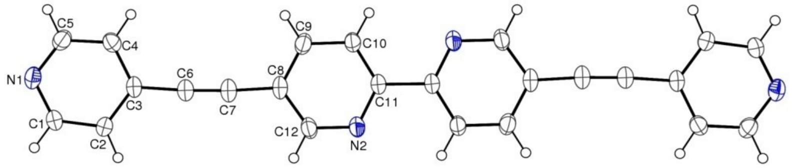

Figure S10. X-ray structures of the 5,5'-bis(pyridin-4-ylethynyl)-2,2'-bipyridine (PYP).

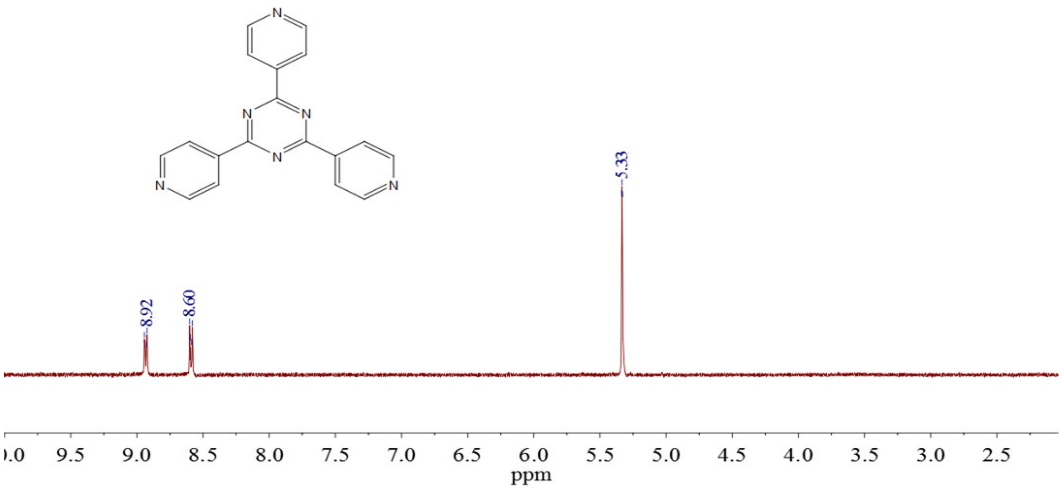

Figure S11. ^{1}H NMR spectrum of TPT in CD_2Cl_2.

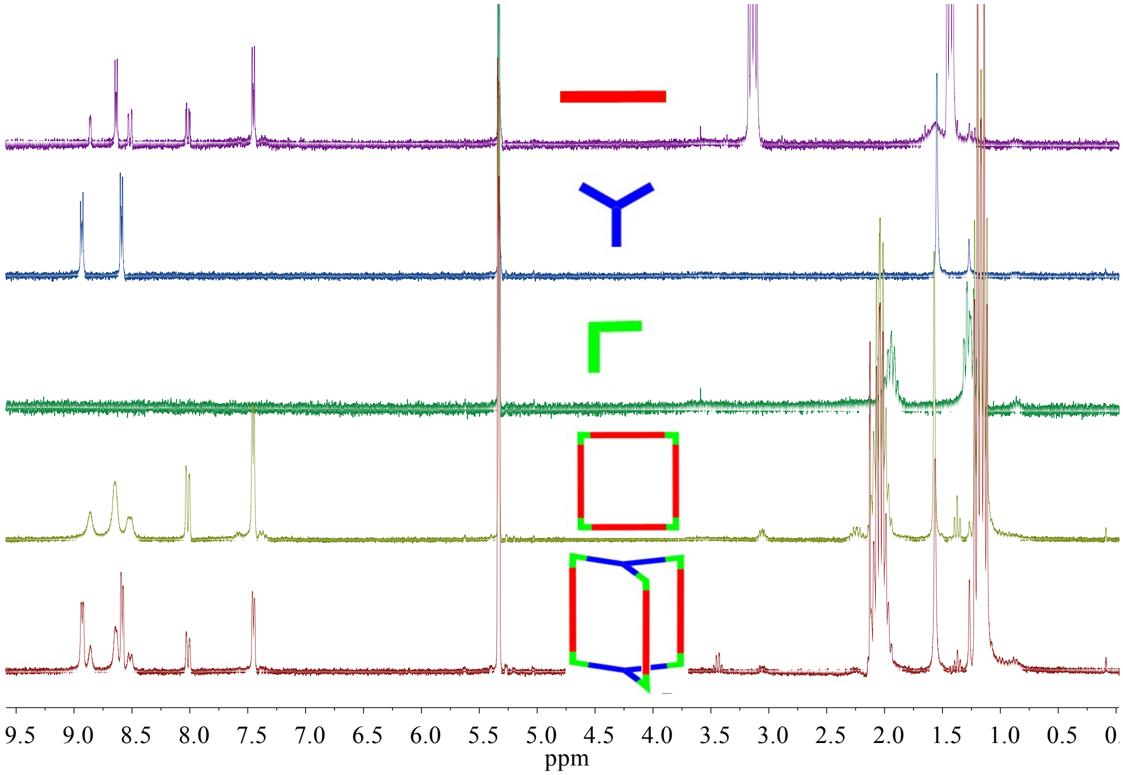

Figure S12. ^{1}H NMR spectra of ligands (PYP and TPT), acceptor, and self-assembled square-like SCC-I and trigonal prisms-like SCC-II in CD_2Cl_2.

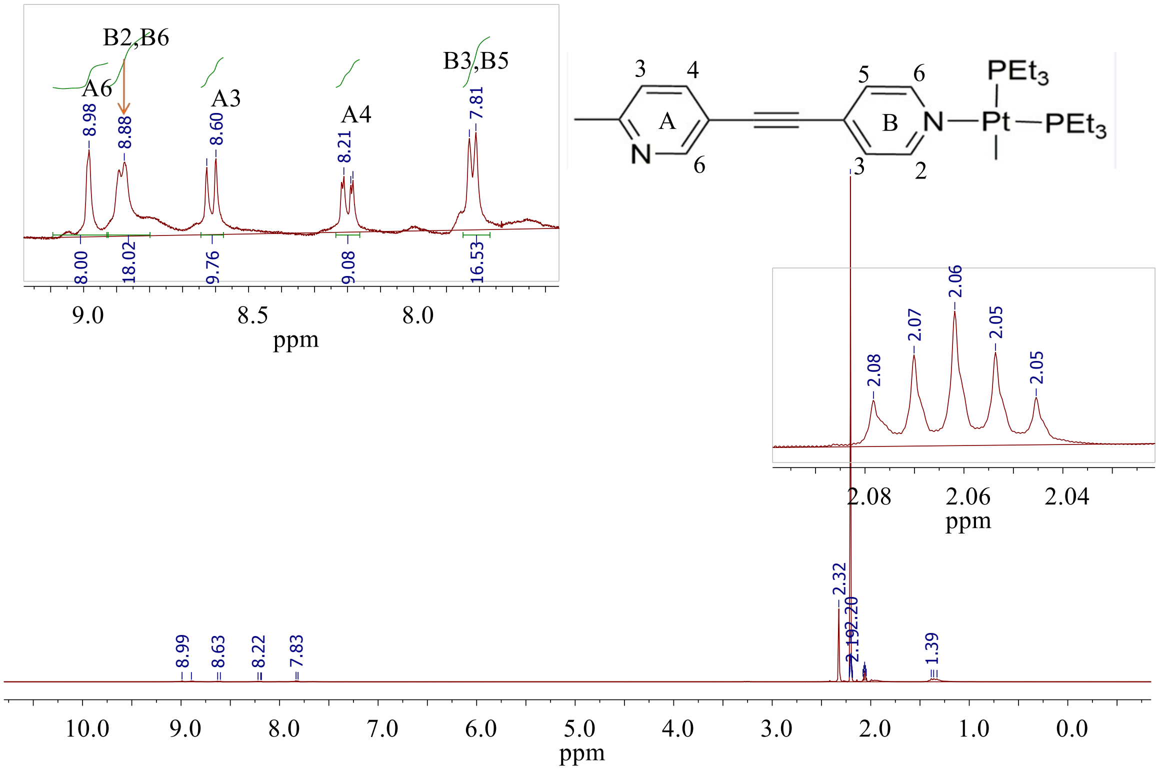

Figure S13. ^{1}H NMR spectrum of square-like SCC-I in acetone-d_6

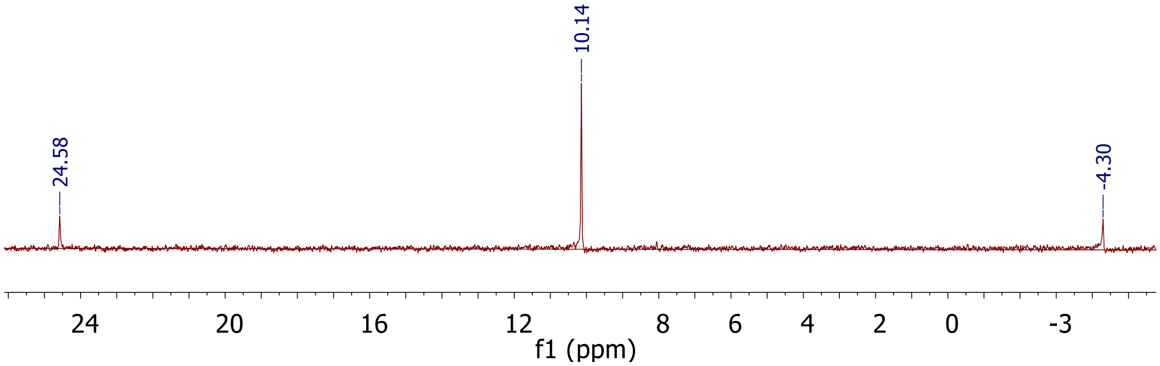

Figure S14. $^{31}P\ \{^{1}H\}$ NMR spectrum of square-like SCC-I in acetone-d_6

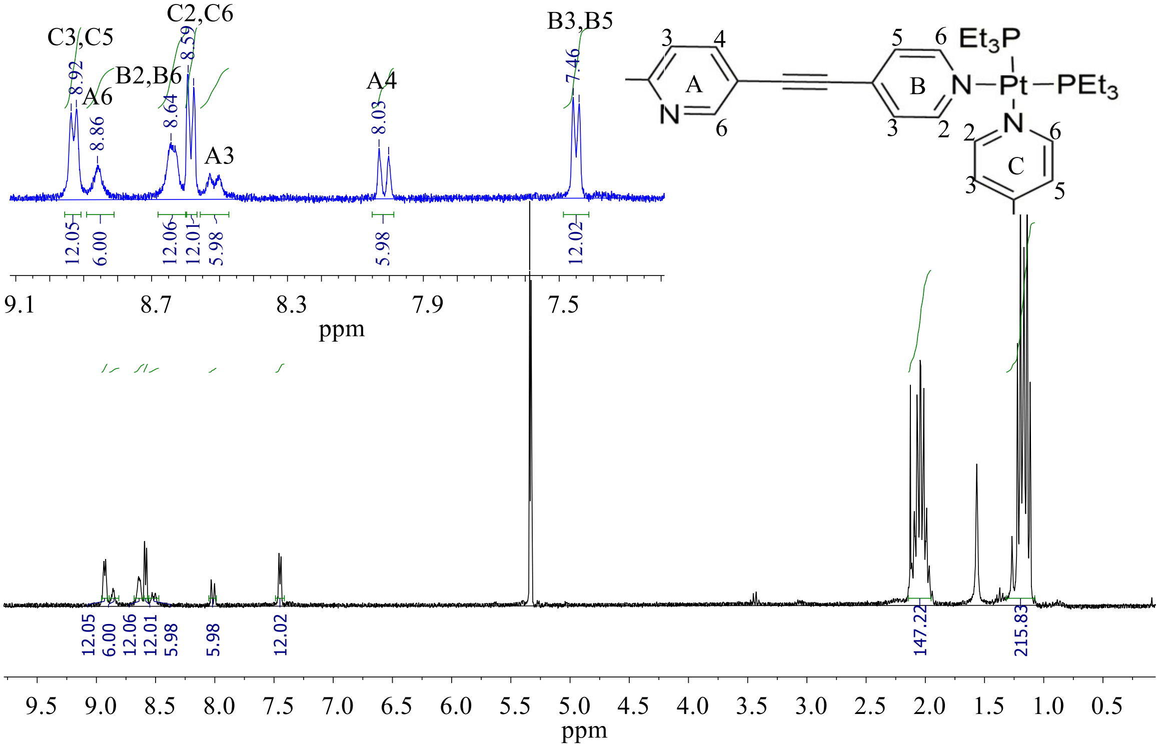

Figure S15. ^{1}H NMR spectrum of trigonal prisms-like SCC-II in CD_2Cl_2.

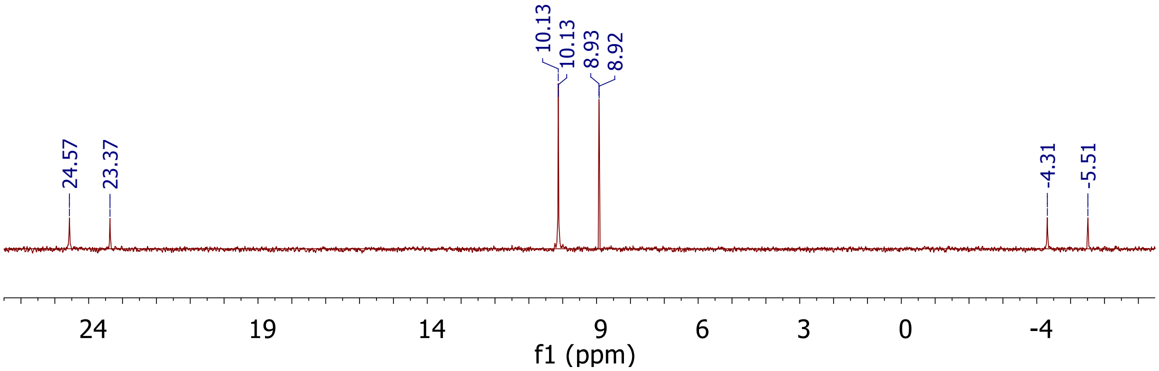

Figure S16. $^{31}P\ \{^1H\}$ NMR spectrum of trigonal prisms-like SCC-II in acetone-$d_{6.}$

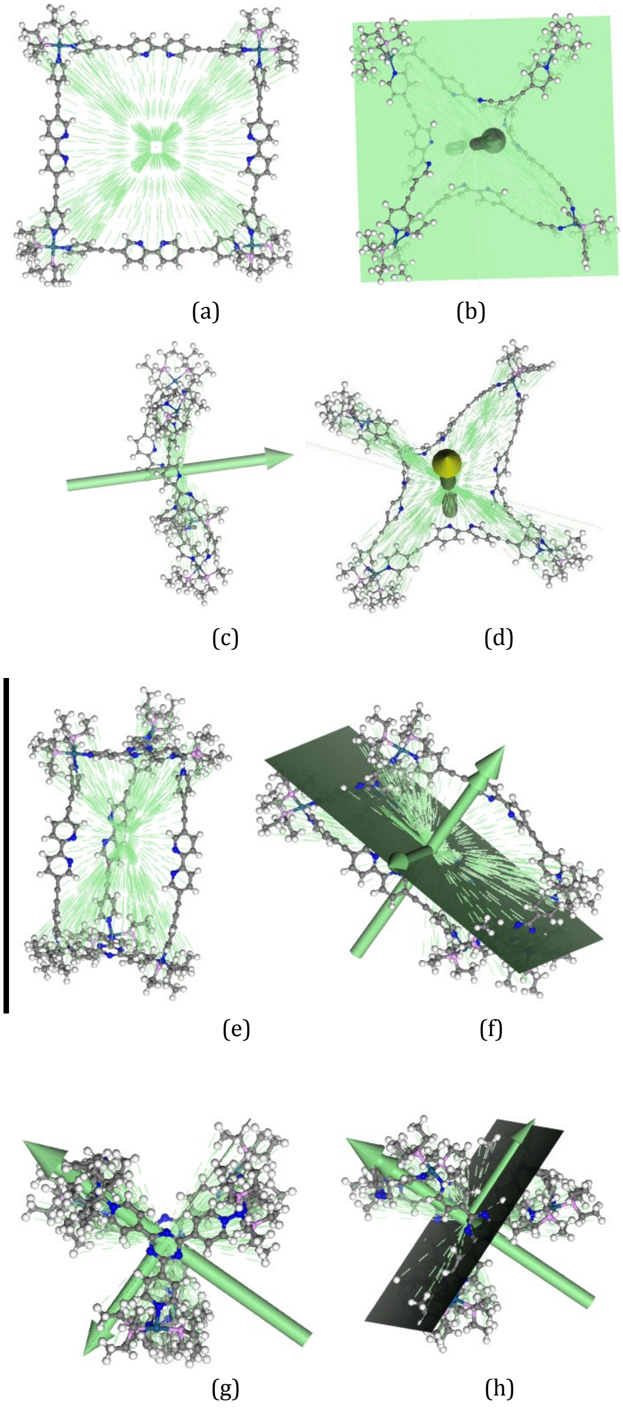
(a) (b)

(c) (d)

(e) (f)

(g) (h)

Figure S17. Proposed structure of the SCC-I (a-d) and SCC-II(e-h) as obtained by Materials Studio via “clean” utility to gain good molecular geometries when added force center.

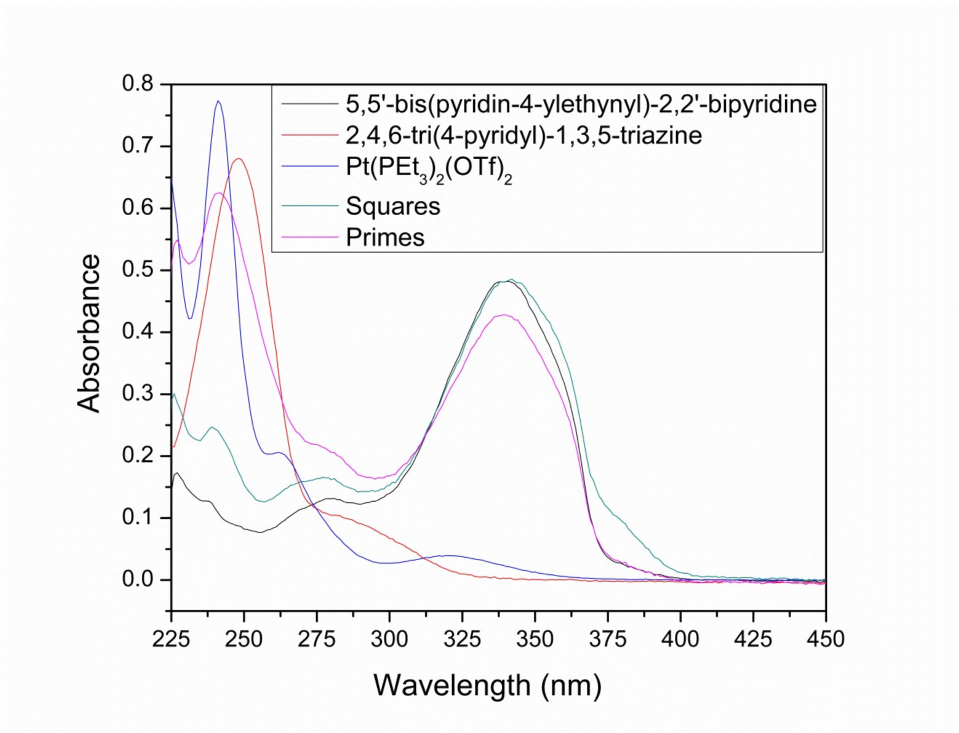

Figure S18. Absorption spectra of different ligands and self-assembled square-like SCC-I and trigonal prisms-like SCC-II (5×10^{-5} M in DCM).

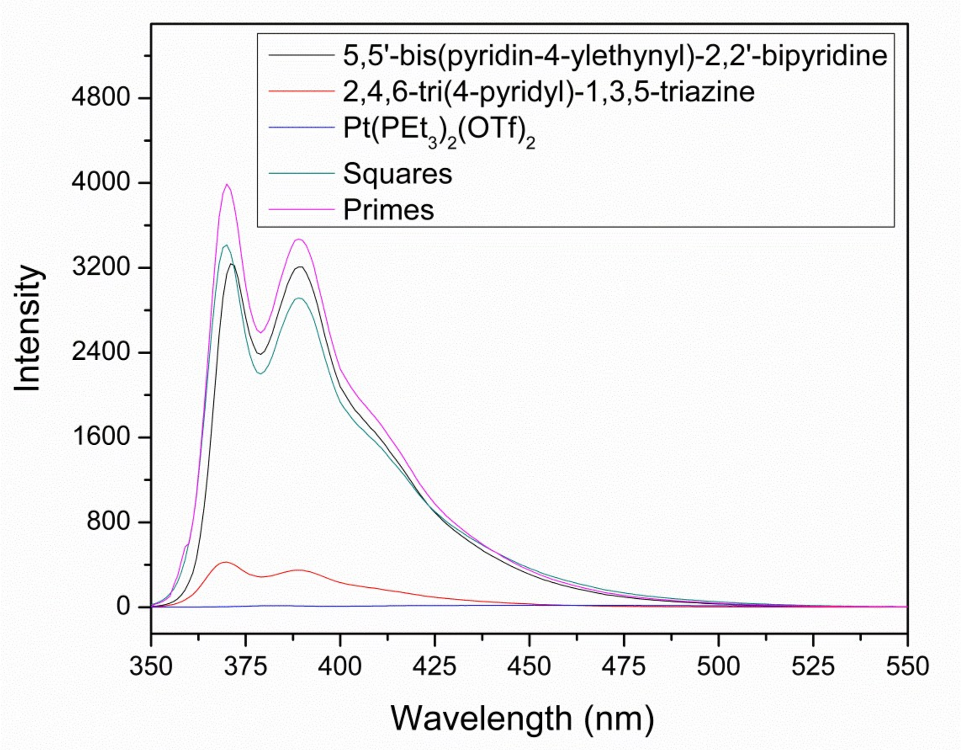

Figure S19. Fluorescence emission spectra (λ_{ex} = 340 nm) spectra of different ligands and self-assembled square-like SCC-I and trigonal prisms-like SCC-II(5×10^{-5} M in DCM).

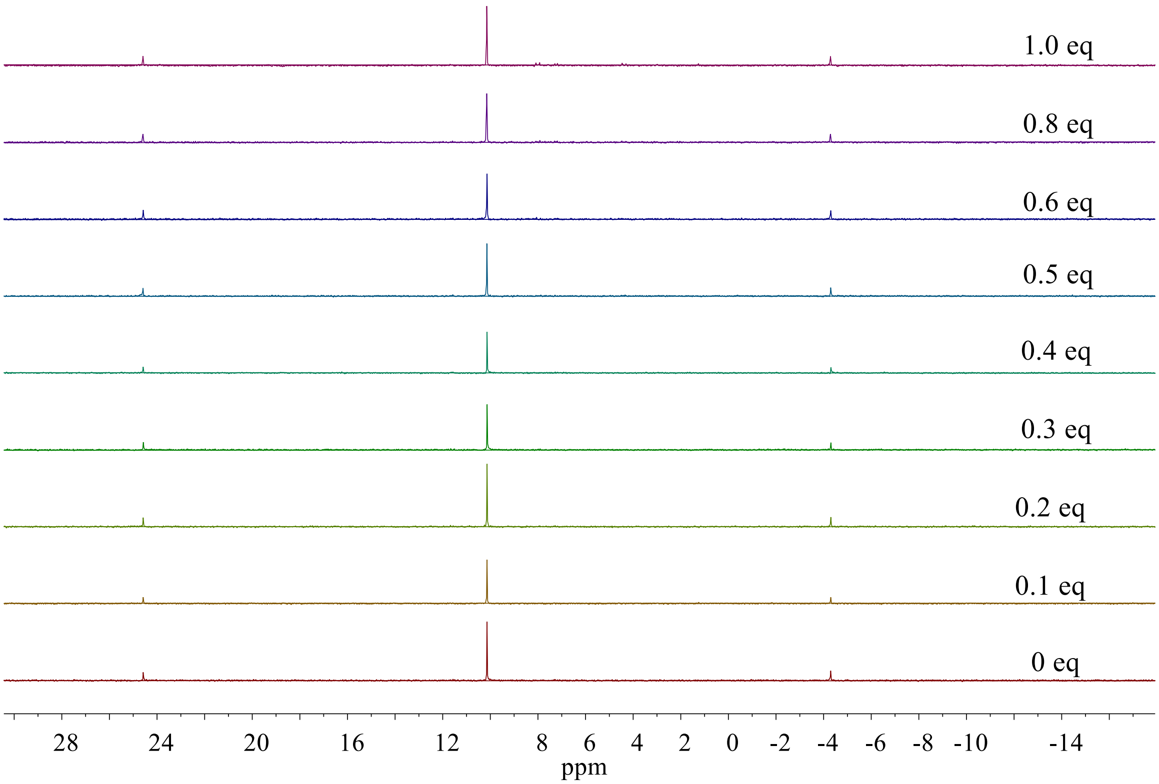

Figure S20. $^{31}P\ \{^{1}H\}$ NMR spectra of Zn^{2+} ion-responsive self-assembled square-like SCC-I in acetone-d_6 with different amount of $Zn(ClO_4)_2$ dissolved in acetone-d_6.

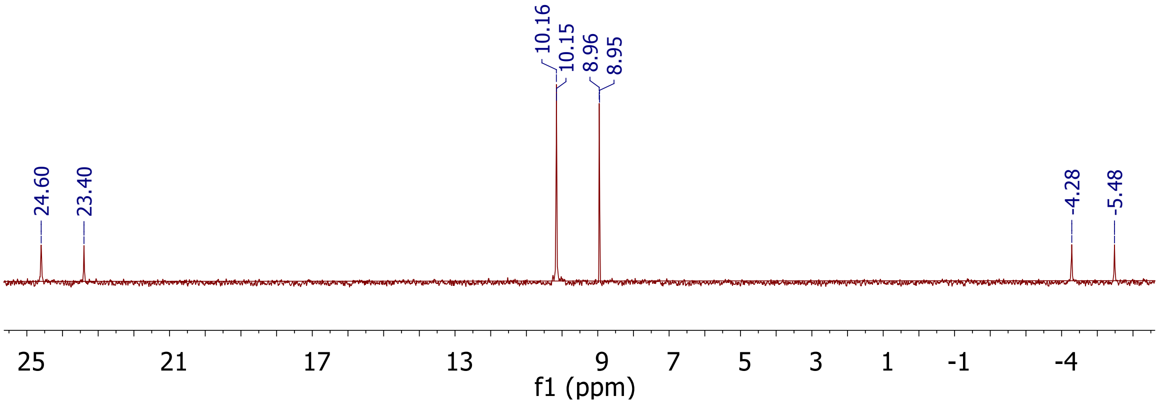

Figure S21. $^{31}P\ \{^{1}H\}$ NMR spectrum of Zn^{2+} ion-responsive self-assembled trigonal prisms-like SCC-II in acetone-d_6 (Zn^{2+} : SCCs = 1:1).

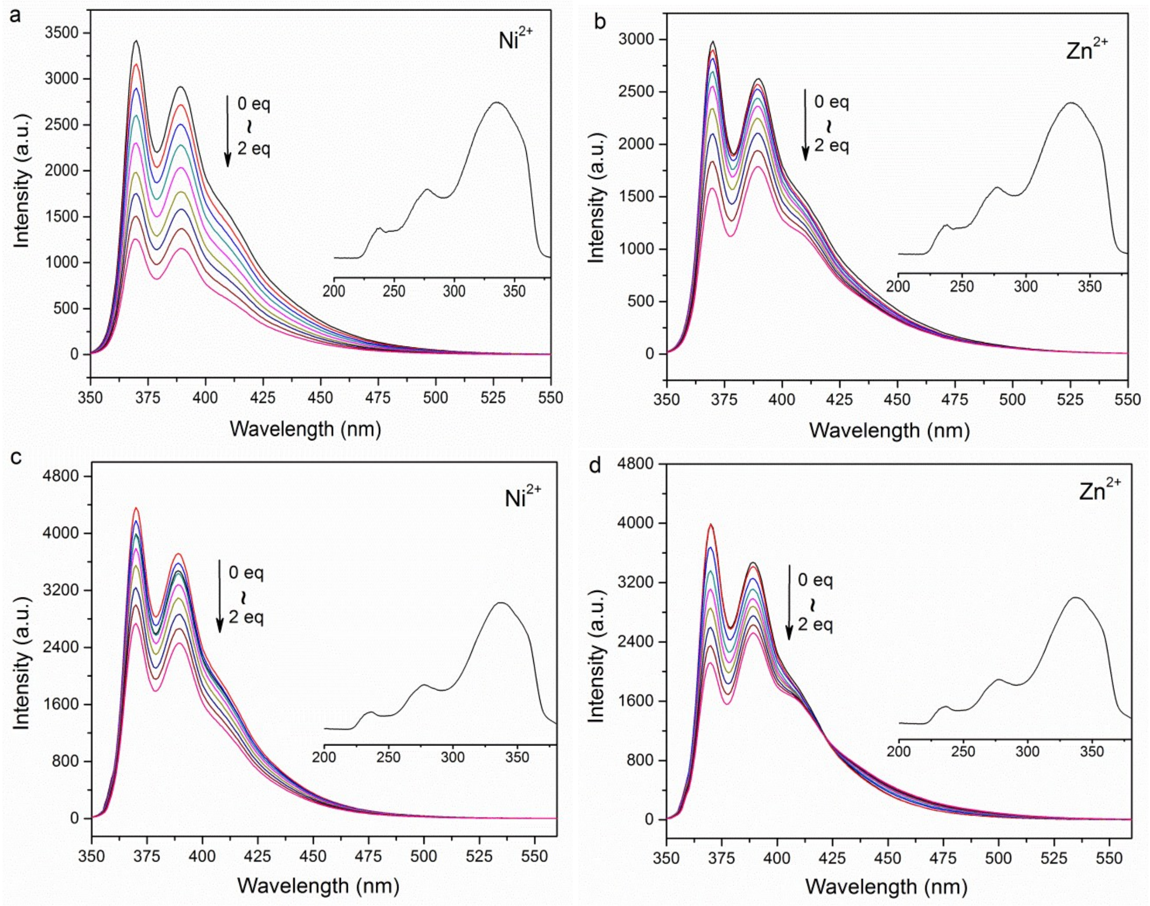

Figure S22. Fluorescence emission spectra (λ_{ex} = 340 nm) spectra of metal-ion-responsive self-assembled SCCs, a and b: Ni^{2+} and Zn^{2+} -square-like SCC-I; c and d Ni^{2+} and Zn^{2+} - trigonal prisms-like SCC-II in DCM(5×10^{-5} M in DCM).

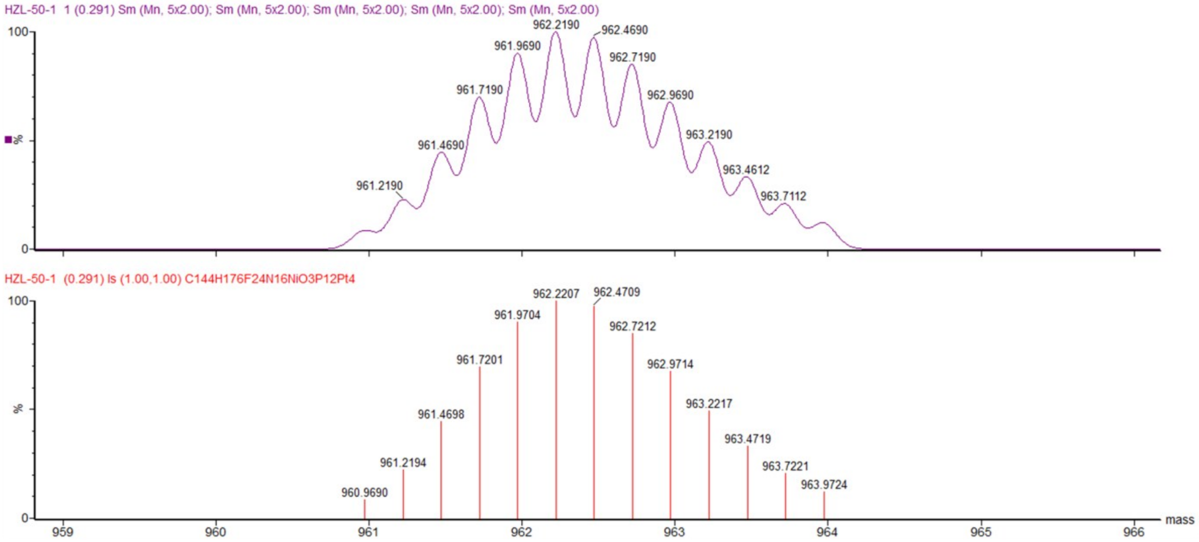

Figure S23. Simulated isotope distribution for species [Ni@SCC-I - 4PF$_6$]$^{4+}$ {m/z=962.2207}(bottom) and experimental isotope distribution for [Ni@SCC-I - 4PF$_6$]$^{4+}${m/z=962.2190} (top).

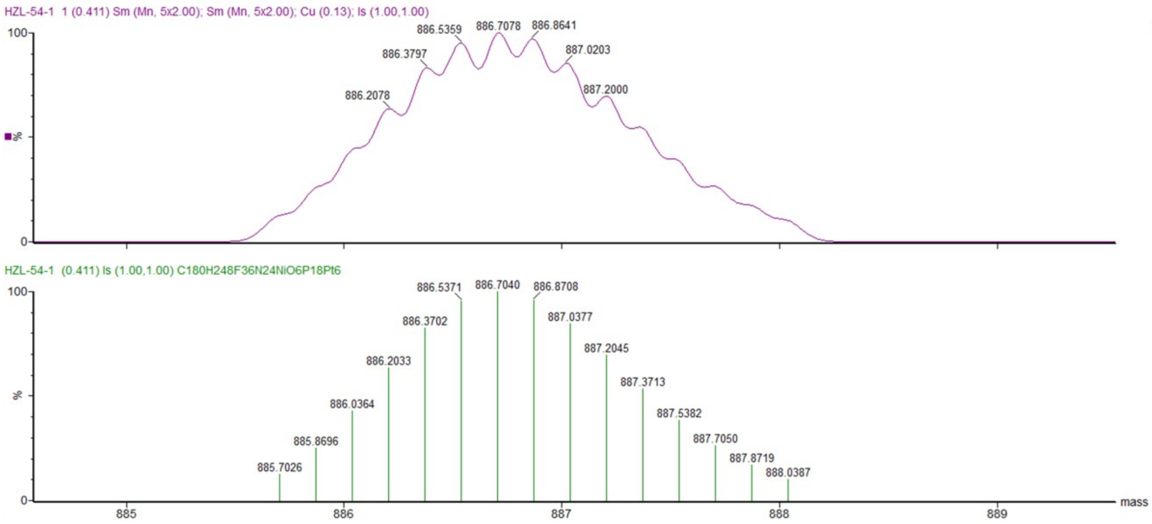

Figure S24. Simulated isotope distribution for species [Ni@SCC-II - 6PF$_6$]$^{6+}$ {m/z=886.7040}(bottom) and experimental isotope distribution for [Ni@SCC-II - 6PF$_6$]$^{6+}${m/z=886.7078} (top).

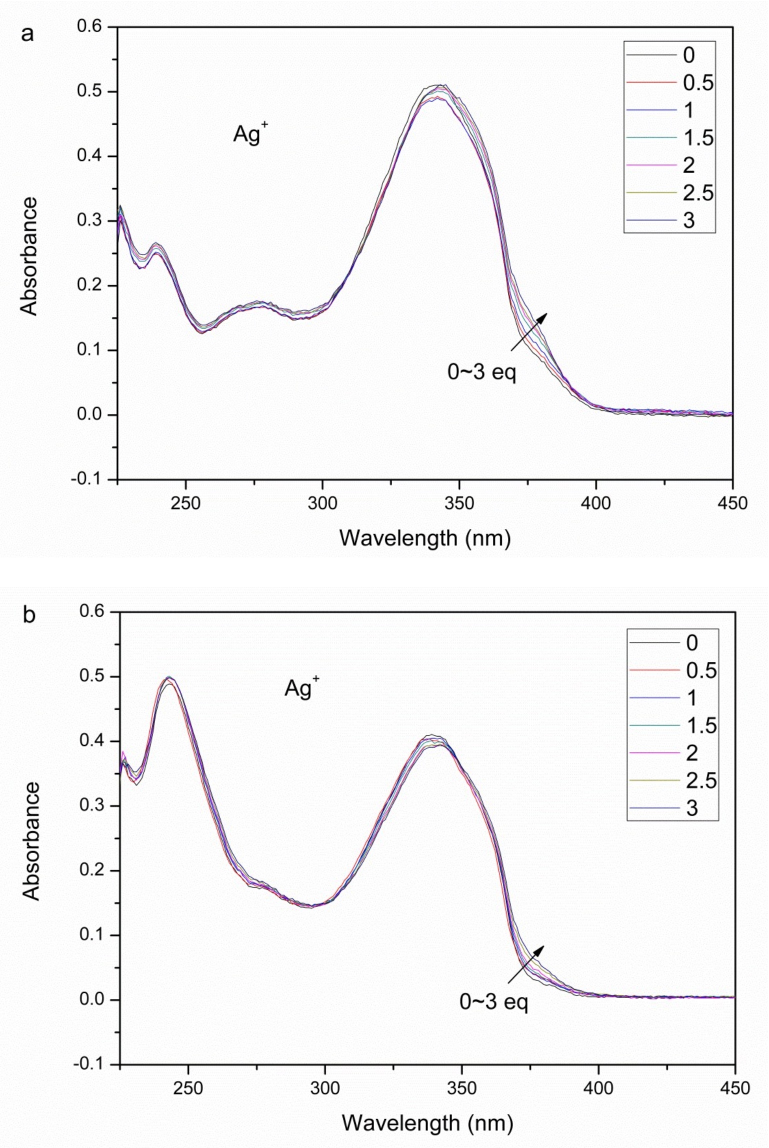

Figure S25. Absorption spectra of Ag^+ ion-responsive self-assembled SCCs: a, square-like SCC-I; b, trigonal prisms-like SCC-II in DCM(5×10^{-5} M in DCM, metal ion : SCCs = 0~3 eq).

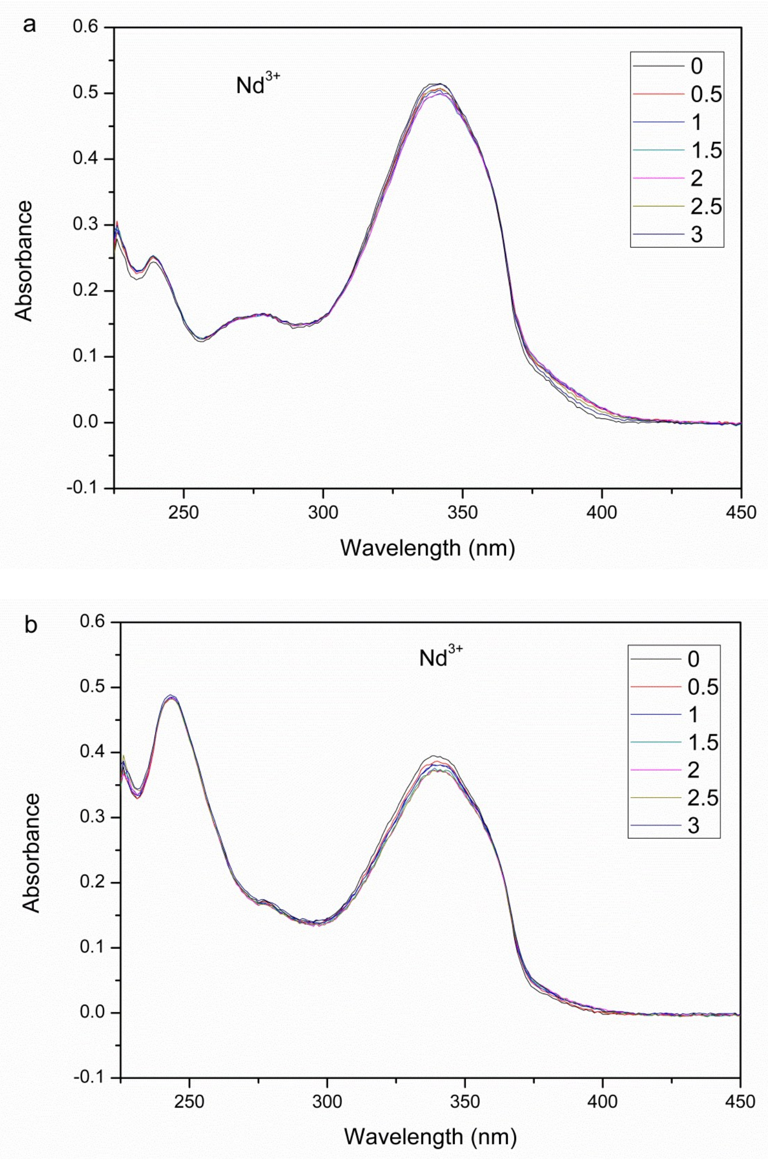

Figure S26. Absorption spectra of Nd^{3+} ion-responsive self-assembled SCCs: a, square-like SCC-I; b, trigonal prisms-like SCC-II in DCM (5×10^{-5} M in DCM, metal ion : SCCs = 0~3 eq).

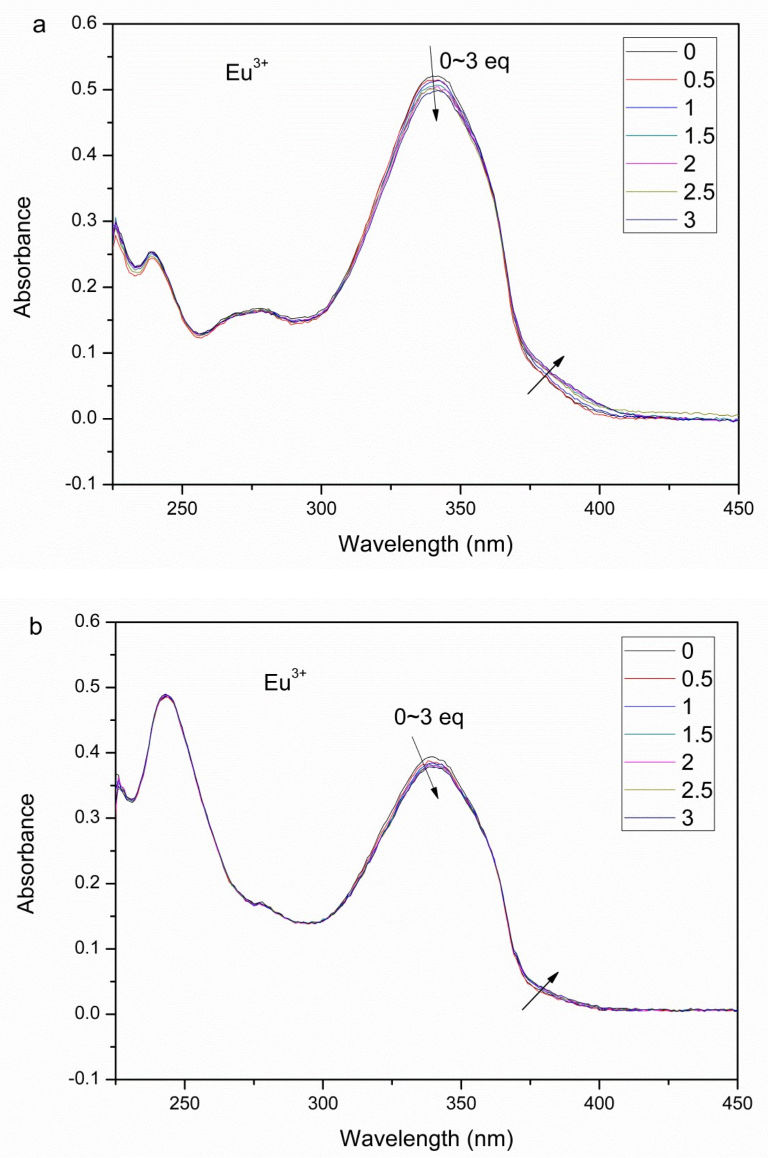

Figure S27. Absorption spectra of Eu^{3+} ion-responsive self-assembled SCCs: a, square-like SCC-I; b, trigonal prisms-like SCC-II in DCM(5×10^{-5} M in DCM, metal ion : SCCs = 0~3 eq).

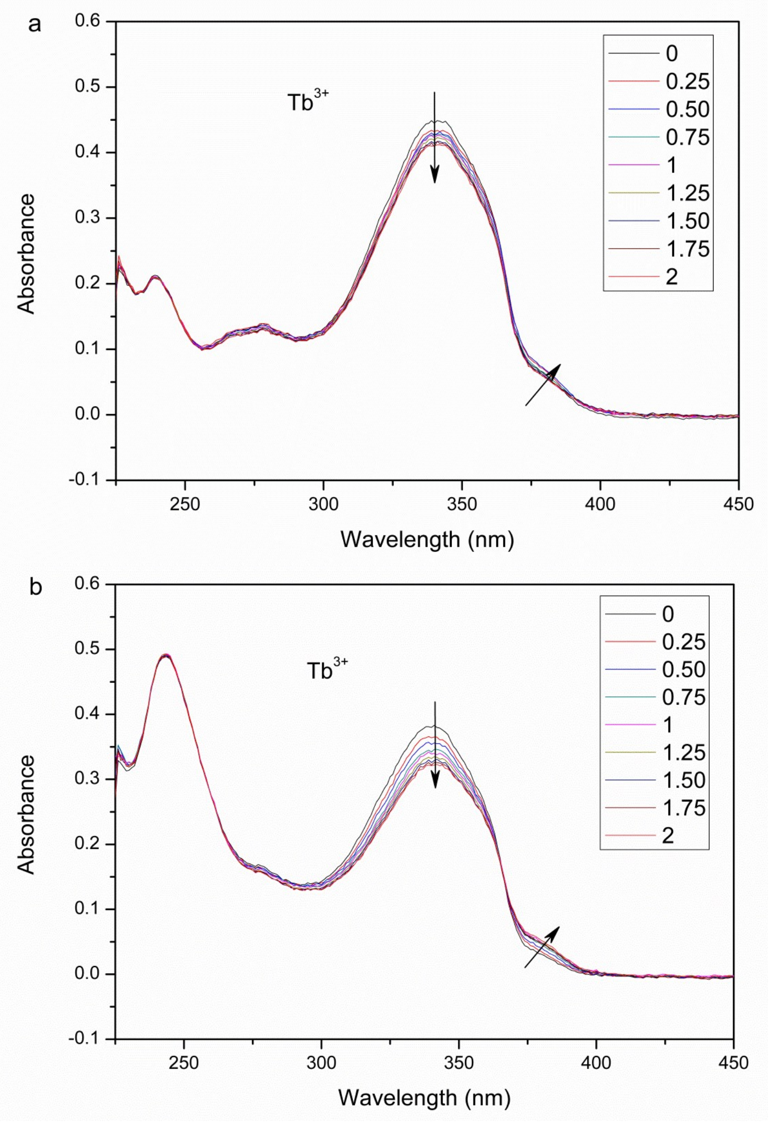

Figure S28. Absorption spectra of Tb^{3+} ion-responsive self-assembled SCCs: a, square-like SCC-I; b, trigonal prisms-like SCC-II in DCM. (5×10^{-5} M in DCM, metal ion : SCCs = 0~2 eq).

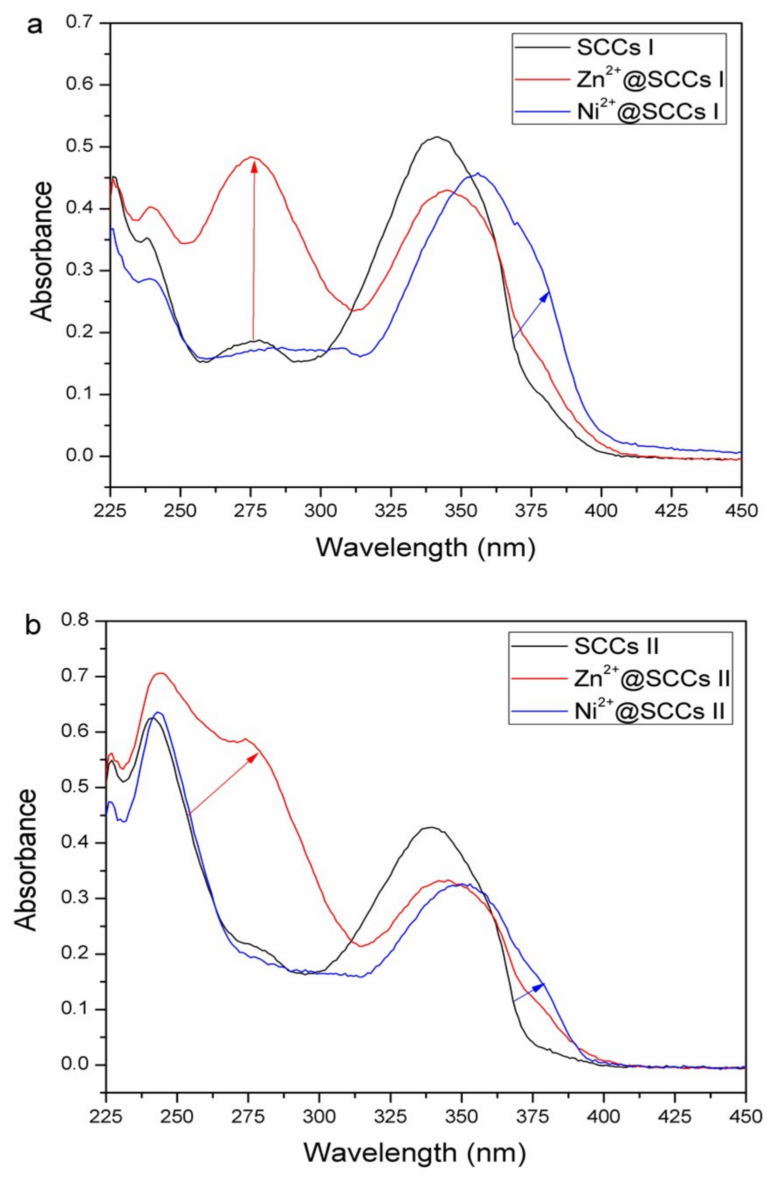

Figure S29. Absorption spectra of Zn^{2+} and Ni^{2}+ion-responsive self-assembled SCCs: a, square-like SCC-I; b, trigonal prisms-like SCC-II in DCM. ($5×10^{-5}$ M in DCM, metal ion : SCCs = 2 eq).

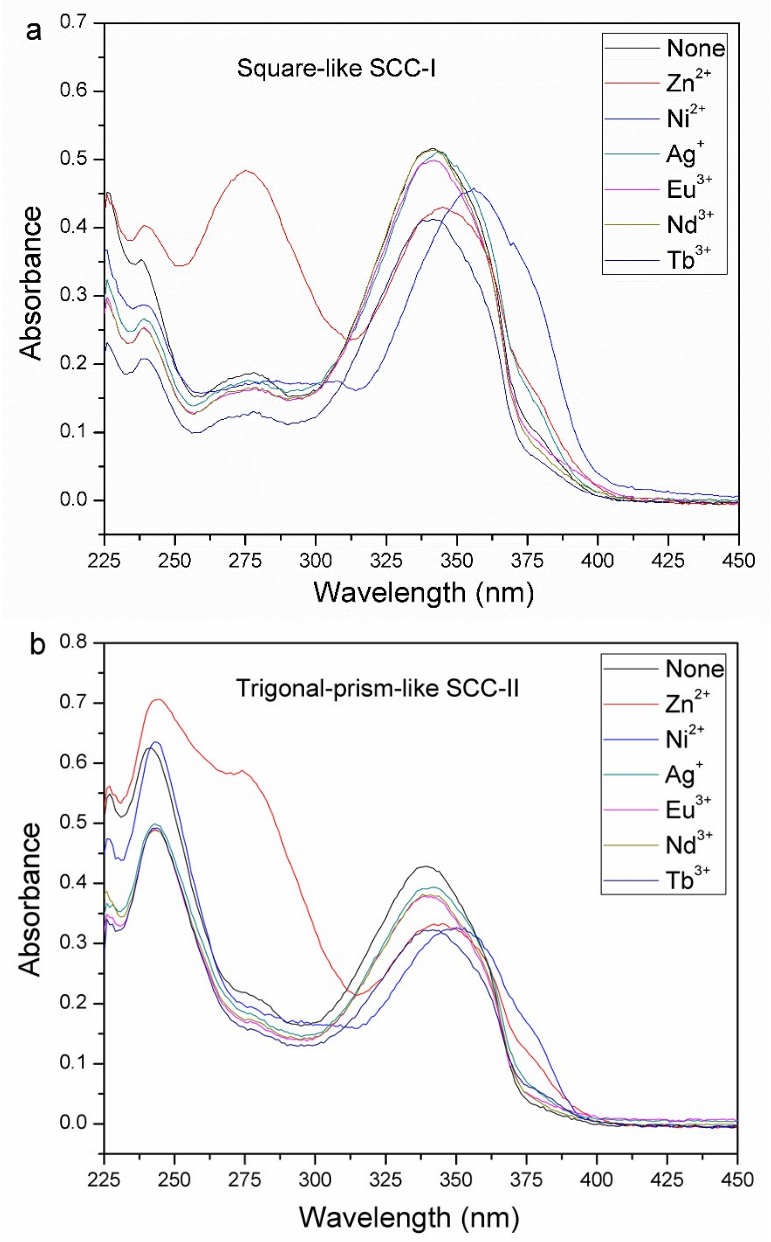

Figure S30. Absorption spectra of different metal ion-responsive self-assembled SCCs: a, square-like SCC-I; b, trigonal prisms-like SCC-II in DCM. (5×10^{-5} M in DCM, metal ion : SCCs = 2 eq).

Supporting Table

Table 1. Crystal data and structure refinement for PYP (pjs249).

Identification code	pjs249
Empirical formula	$C_{24}H_{14}N_4$
Formula weight	358.39 g/mol
Temperature	150(2) K
Wavelength	0.71073 Å
Crystal system	Monoclinic
Space group	P 1 21/n 1

Unit cell dimensions	a = 8.5761(7) Å;
	b = 5.7765(5) Å;
	c = 18.0007(14) Å.
	α = 90°;
	β = 93.358(3)°;
	γ = 90°

Volume	890.22(13) $Å^3$
Z	2
Density (calculated)	1.337 g/cm^3
Absorption coefficient	0.082 mm^{-1}
F(000)	372
Crystal size	0.13 x 0.17 x 0.45 mm^3
Theta range for data collection	2.27 to 26.48°
Index ranges	-10<=h<=7, -7<=k<=7, -22<=l<=17
Reflections collected	5273
Independent reflections	1810 [R(int) = 0.0298]
Completeness to theta = 26.48°	98.4%
Absorption correction	Multiscan
Max. and min. transmission	0.9900 and 0.9640
Refinement method	Full-matrix least-Squares on F^2
Data / restraints / parameters	1810 / 0 / 127
Goodness-of-fit on F^2	1.084
Final R indices [I>2sigma(I)]	R1 = 0.0479, wR2 = 0.1370
R indices (all data)	R1 = 0.0613, wR2 = 0.1479
Largest diff. peak and hole	0.380 and -0.188

References

1. Armarego, W. L. F.; Chai, C. L. L. Purification of Laboratory Chemicals, 6th ed.; Butterworth-Heinemann: Oxford, U.K., **2009**.

2. Ayme, *J.*-F.; Beves, *J*. E.; Leigh, D. A.; McBurney, R. T.; Rissanen, K.; Schultz, D., A synthetic molecular pentafoil knot. *Nat. Chem.* **2012,** *4* (1), 15-20.

3. Resendiz, M. *J*. E.; Noveron, *J*. C.; Disteldorf, H.; Fischer, S.; Stang, P. *J*., A Self-Assembled Supramolecular Optical Sensor for Ni(II), Cd(II), and Cr(III). *Org. Lett.* **2004,** *6* (5), 651-653.

4. Li, M.-X.; Miao, Z.-X.; Shao, M.; Liang, S.-W.; Zhu, S.-R., Metal-Organic Frameworks Constructed from 2,4,6-Tris(4-pyridyl)-1,3,5-triazine. *Inorg. Chem.* **2008,** *47* (11), 4481-4489.